Spectroscopy of Herbig-Haro Objects in Perseus: Physical Conditions and Kinematics

Author: Queralt Balada Armengol.
Advisor: Maria Rosario López Hermoso
Facultat de Física, Universitat de Barcelona, Diagonal 645, 08028 Barcelona, Spain.*

Abstract: Through calculating emission-line ratios of Herbig-Haro (HH) objects' optical spectra, we can perform an analysis of their physical and kinematic conditions. The purpose of this work is to obtain such diagnosis for the HH objects located in the Perseus molecular cloud. Even though not enough data are available to complete a study of the region, 45 objects were studied and divided into two categories according to their degree of excitation; a prevalence for high/intermediate excitation was found in the sample, with 36/45 objects belonging to that group. It was also noticed that the ionization fraction and shock velocity values were lower for the low excitation objects, and no significant correlation was found between the values of radial velocity and degree of excitation.

I. INTRODUCTION

In the star formation process, the young stellar object (YSO) interacts heavily with the environment. As the molecular cloud leading to the future star has a much higher mass than the latter, powerful mass-loss processes take place, in addition to the mass-accretion through gravitational collapse.

The ejection of mass is carried out through different phenomena (stellar winds, molecular outflows, jets, etc.). In this project we're interested in the material expelled at high speeds, typically in both directions perpendicular to the accretion disk, that creates a bipolar outflow of highly collimated gas, i.e. highly collimated stellar jets.

One of the manifestations of this outflow activity are Herbig-Haro (HH) objects, which are generally small nebulae that emit in the visible part of the spectrum and have very characteristic emission lines.

These were discovered independently by George Harbig and Guillermo Haro in the early 1950s, and were then thought to be luminous nebulae containing stars in formation. It was later discovered that they were shock waves or knots resulting from the interaction of the highly collimated gas, ejected from the YSO, with the environment or with the same gas at a different speed.

Due to various reasons like the different evolutionary stages of the HH objects, their environments, the chaotic nature of shocks, etc. there is a very large array of morphologies. The better-known ones are the bow shock and the highly collimated jet. In the case of HH jets, they're typically formed by a string of knots, where faster moving gas shocks with the slower moving gas, and in many cases they point to a bow shock HH.

The study of these objects is interesting as in gives insight into the mass-ejection process in the process of star formation, which then can be used to understand better the mass-accretion process.

The recombination process behind the shocks produces the emission line spectrum of the HH objects, resulting in permitted and forbidden lines corresponding to optical wavelengths and some weak emission on the blue and UV region.

It is particularly interesting that there have been found simultaneously low excitation lines such as [SII] and [OI] and high excitation ones such as [OIII].

Through the analysis of the emission line fluxes we can study the physical conditions such as electron density, degree of excitation and ionization, etc. as well as their kinematic properties. The purpose of this work is to make a diagnosis of the aforementioned conditions of some HH objects belonging to the Perseus star forming region, which we've found through the paper [1].

II. DATA COMPILATION

The collection of HH objects, belonging to the Perseus molecular cloud, used for the diagnosis have been obtained through the tables 2 and 3 of the article [1].

We've looked for their spectra in the SIMBAD database [2], which compiles the bibliography of all known HH objects.

The first thing we've noticed is the scarcity of spectroscopical observations in the optical region. Out of the 184 objects in our sample, only enough data were found, to do the spectroscopical analysis, for 45 (see Table I, first column). And of those, 32 only have data for the [SII] (6717+6731) and Hα lines.

With the found fluxes, we've calculated the [SII]/Hα (Table I, column 2) and the [SII]6717/6731 (Table I, column 3) ratios, as well as the [NII]/Hα for the 13 objects for which the information was available.

We've also assembled the data from their radial velocities (Table I, column 7).

Additionally, with the help of theoretical models, we've performed the diagnosis of the objects' physical and kinematic conditions, which I'll comment on in the following section.

III. RESULTS

The results of the obtained diagnosis are summarized and presented in Table I.

A. Physical conditions

To obtain the degree of excitation, we've used the [SII] (6717+6731)/Hα ratios. We've classified our objects into two categories (high/intermediate and low excitation) according to the criterion in [3]: The low excitation objects correspond to those with a line ratio of [SII] (6717+6731)/H$\alpha \leq 1{,}5$ and those with a smaller ratio correspond to high or intermediate excitation spectra. The resulting classification is shown in Table I, column 3.

Using also the Hα/[NII](6584) flux ratio, [3] defines some diagnostic diagrams to visualize the excitation degree of the objects. We've built a diagram of this kind with the objects of our sample of which we have the necessary data available.

* Electronic address: tfgac@ub.edu

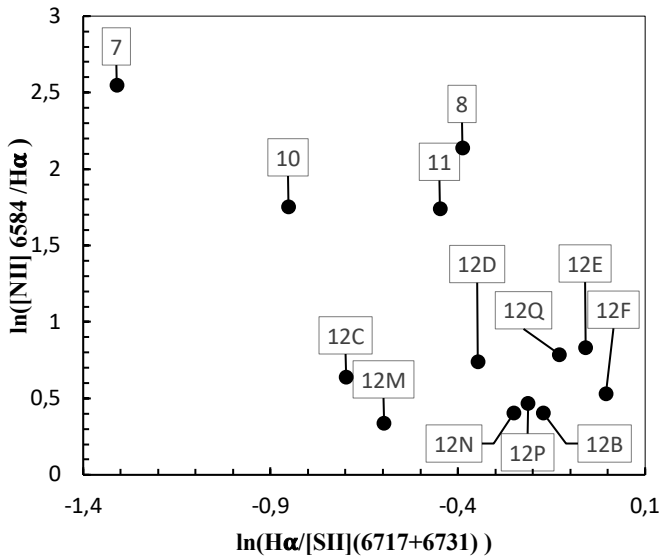

FIG. 1: Herbig-Haro objects distributed according to ln([NII] 6584 Å /H**α**) vs. ln(H**α**/[SII](6717+6731)) . Based on Fig.2 from [3].

Regarding the tracer of electron density (n_e), we've used the [SII]6717/6731 intensity ratios. With these and by using Figure 5.3 of the Osterbrock book [5], we've obtained the results seen in Table I, column 5. These density values have been estimated for a temperature of T=10000K, if the temperature of our objects differs, these values should be taken as $n_e(10^4/T)^{1/2}$. We have also built a diagnostic diagram to help visualize this, following diagrams from [4].

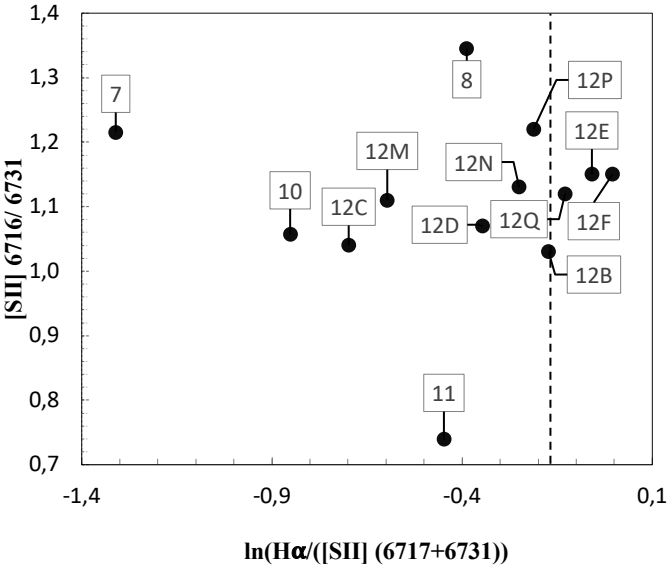

FIG. 2: Herbig-Haro objects distributed according to their tracer of electron density vs. degree of excitation. The line at approximately -0,28 ln(H**α**/([SII] (6717+6731)) separates the low excitation objects (left) from the high/intermediate excitation objects (right), according to the aforementioned criterion. Based on figures from [4].

To calculate the ionization fraction (what percentage of the gas is ionized), we've used the [SII] (6717+6731)/H**α** ratios as well as the [OI] /H**α** ratios for the few we had the [OI] line flux available. The theoretical models used for these calculations are those in Fig. 3 and Fig. 4 of the article [6]. We've used the models corresponding to density values of n_0=100 cm^{-3} and n_0=1000 cm^{-3}, and magnetic fields ranging from 0 μG o 1000μG, as these are the values expected for HH objects, to find the range of possible degrees of ionization. The resulting information is presented in Table I, column 6.

For a few objects whose [SII] (6717+6731)/H**α** ratio is 0,1, there are no ionization fraction values for n_0=100cm^{-3} , according to the models used.

B. Kinematic conditions

The radial velocity is obtained from the emission of the H**α** line, but our results are taken from the articles cited in the Table I, and the values are shown in column 7 from that same table.

The shock velocity of HH objects gives us an idea about the force of the shock between the jet's high-speed gas and the surrounding environment. These shocks can be between faster and slower moving or gas or the jet and the still unperturbed ambient medium. To calculate this, we've used the low excitation forbidden lines [SII] and [OI], as well as H**α** to work with the [SII] (6717+6731)/H**α** and [OI]/H**α** line ratios, and the models shown in Fig. 8 and Fig.9 of [6]. We've used again the values corresponding to densities of n_0=100 cm^{-3} and n_0=1000 cm^{-3}, and magnetic fields from 0 μG o 1000μG to obtain the range of shock velocity values for the HH objects (Table I, column 8).

In the cases where the [SII] (6717+6731)/H**α** quotient is 0,1, the theoretical models do not give possible shock velocities for n_0=100cm^{-3}, in the range of magnetic fields analysed. This is probably due to the fact that this high degree of excitation can't be obtained by such low density objects.

IV. DISCUSSION

Using the criterion mentioned in section III. A, we've divided the objects of our sample into two main categories, according to their degree of excitation (high/intermediate or low). It is noticeable that a much higher percentage of the studied objects belong to the high/intermediate excitation spectra objects group (36/45) than in the low excitation group (9/45). While keeping that in mind, we've assembled a table for the statistics of each category.

Average Values and Range for High/Intermediate Excitation HH Objects

Number of Objects: 36

	Max	Min	Average	Standard deviation
n_e (cm^{-3})*	810	200	462	196
Ion. Frac.	0,4	0,05	0,19	0,1
V_r (km/s)	110	-63	-1,8	7,3
V_s (km/s)	75	40	53	9,5

TABLE II: Table showing the maximum and minimum values, the average and the standard deviation for the electron density tracer, the ionization fraction, the radial velocity and the shock velocity for high/intermediate excitation objects.

*The electron density values have been calculated with only 6 objects of similar characteristics, as they were the only ones with the data available.

Average Values and Range for Low Excitation HH Objects

Number of Objects: 9

	Max	Min	Average	Standard deviation
n_e (cm^{-3})*	1900	440	724	599
Ion. Frac.	0,065	0,015	0,025	0,008
V_r (km/s)	3	-175	-46	57
V_s (km/s)	38	20	30	4,4

TABLE III: Table showing the maximum and minimum values, the average and the standard deviation for the electron density tracer, the ionization fraction, the radial velocity and the shock velocity for low excitation objects.
*The electron density values have been calculated with only 7 objects.

As seen in the tables, the electron density values appear to be higher for the low excitation objects, nonetheless, this cannot be taken as a conclusion from these data, due to the extremely small fraction of high/intermediate excitation objects with n_e information.

The noticeably differing characteristics between the two groups are the ionization fraction and the shock velocity. They show significantly higher values in the high/intermediate excitation category.

On the other hand, there doesn't seem to be a correlation between the radial velocity and the degree of ionization, or at least our data are not concluding.

V. CONCLUSIONS

- The lack of spectroscopic observations in the optical region has resulted in not having enough data to perform a complete study of the HH objects in the Perseus region.
- Low excitation HH objects are less prevalent than high or intermediate excitation objects in our sample.
- On average, the values of ionization fractions and shock velocities are higher for high/intermediate excitation objects. Whereas radial velocities show no clear differences with the degree of excitation, and the data on electron density is inconclusive.

VI. APPENDIX

In the next page we present our results summarized in Table I.

Acknowledgments

I'd like to thank my advisor for her enormous help, my mother for her support and advice, my father for his support and my friends for their advice.

[1] Josh Walawander, John Bally and Bo Reipurth, «Deep Imaging Surveys of Star-forming Clouds. III. Herbig-Haro Objects in the Perseus Molecular Cloud,» *The Astronomical Journal,* pp. 2311-2312, 2005.

[2] «SIMBAD Astronomical Database-CDS (Strasbourg),» [Online].

Available: http://simbad.u-strasbg.fr/simbad/

[3] A.C. Raga, K.-H. Böhm and J. Cantó, «A Compilation of Optical Spectrophotometry and its Tentative Interpretation», *Rev. Mex. Astron. Astrofis.,32,* pp. 161-174, 1996.

[4] J. Cantó, in *Investigating the Universe*, Dodrecht:Reidel, F. Khan, 1981, p. 95.

[5] D. E. Osterbrock and G.J. Ferland, *Astrophysics of Gaseous Nebulae and Active Galactive Nuclei,* University Science Books, Mill Valley, California, USA, pp. 134, 1989.

[6] Patrick Hartigan, Jon A. Morse and John Raymond, «Mass-loss Rates, Ionization Fractions, Shock Velocities and Magnetic Fields of Stellar Jets,» *The Astrophysical Journal, 436,* pp. 125-143, 1994.

[7] A. Noriega-Crespo, A. Cotera, E. Young and H. Chen, «Hubble Space Telescope NICMOS Images of the HH 7/11 Outflow in NGC 1333,» *The Astrophysical Journal, 580,* pp. 959-968, 2002.

[8] J. Bally, David Devine, and Victoria Alten, «New Herbig Haro Flows in L1448 and L1455» *The Astrophysical Journal, 478,* pp. 603-613, 1997.

[9] E.R. Hovannessian, T.Yu. Magakian, and T.A. Movessian, «Spectral Study of the Object HH 12» *Astrophysics, 49,* pp. 63-69, 2006.

[10] Robert W. Goodrich, «New Observations of Herbig-Haro objects and Related Stars» *The Astronomical Journal, 92,* 4, 1986.

TABLE I

Physical conditions and kinematics of Herbig-Haro Objects

HH	[SII]/Hα	Degree of excitation	[SII] 6716/ 6731	n_e**	Ionization fraction*	V_r	V_s*
				cm^{-3}	%[min,max]	km/s	km/s
280A	0,6	High/intermediate	…	…	[0.1,0.15]	-45	[45,50]
280B	0,7	High/intermediate	…	…	[0.08,0.12]	…	[45,50]
280C	0,3	High/intermediate	…	…	[0.19,0.3]	…	[53,63]
267A	0,5	High/intermediate	…	…	[0.12,0.15]	-50	[50,55]
267B	0,3	High/intermediate	…	…	[0.19,0.3]	0	[53,63]
267C	0,2	High/intermediate	…	…	[0.25,0.4]	-63	[60,72]
267D	0,3	High/intermediate	…	…	[0.19,0.3]	…	[53,63]
268A	0,2	High/intermediate	…	…	[0.25,0.4]	29	[60,72]
268B	0,4	High/intermediate	…	…	[0.12,0.25]	…	[50,55]
193A	0,3	High/intermediate	…	…	[0.19,0.3]	-18	[53,63]
193B	0,4	High/intermediate	…	…	[0.12,0.25]	10	[50,55]
193C	0,4	High/intermediate	…	…	[0.12,0.25]	-10	[50,55]
194A	0,2	High/intermediate	…	…	[0.25,0.4]	66	[60,72]
194B	0,2	High/intermediate	…	…	[0.25,0.4]	66	[60,72]
194C	0,1	High/intermediate	…	…	[…,0.4]***	110	[…,75]***
195A	0,4	High/intermediate	…	…	[0.12,0.25]	-35	[50,55]
195B	0,2	High/intermediate	…	…	[0.25,0.4]	-31	[60,72]
195C	0,2	High/intermediate	…	…	[0.25,0.4]	…	[60,72]
195D	0,4	High/intermediate	…	…	[0.12,0.25]	-16	[50,55]
195E	0,7	High/intermediate	…	…	[0.08,0.12]	-35	[45,50]
196A	0,2	High/intermediate	…	…	[0.25,0.4]	0	[60,72]
196B	0,1	High/intermediate	…	…	[…,0.4]***	0	[…,75]***
196C	0,1	High/intermediate	…	…	[…,0.4]***	-35	[…,75]***
197	0,8	High/intermediate	…	…	[0.08,0.11]	-33	[45,50]
278A	0,8	High/intermediate	…	…	[0.08,0.11]	…	[45,50]
278B	0,8	High/intermediate	…	…	[0.08,0.11]	…	[45,50]
278C	2,3	Low	…	…	[0.027,0.03]	…	[25,35]
317	0,7	High/intermediate	…	…	[0.08,0.12]	15/35	[45,50]
279A	1,7	Low	…	…	[0.02,0.03]	-46	[33,38]
279B	1,1	High/intermediate	…	…	[0.05,0.09]	…	[40,42]
279C	1,1	High/intermediate	…	…	[0.05,0.09]	…	[40,42]
318	0,3	High/intermediate	…	…	[0.19,0.3]	…	[53,63]
11	1,6	Low	0,7	1900	[0.02,0.03]/[0.02,0.03]	-175	[33,38]/[20,30]
10	2,3	Low	1,0	810	[0.027,0.03]/[0.02,0.03]	-35	[25,35]/[20,30]
8	1,5	Low	1,3	100	[0.02,0.03]/[0.02,0.065]	-57	[33,38]/[30,35]
7	3,7	Low	1,2	200	[…,0.015]/[0.02,0.03]	-51	[25,30]/[20,29]

12B	1,2	High/intermediate	1,0	810	[0.05,0.09]	5	[40,42]
12C	2,0	Low	1,0	810	[0.025,0.03]	-5	[23,30]
12D	1,4	Low	1,0	810	[0.02,0.03]	3	[33,38]
12E	1,1	High/intermediate	1,1	440	[0.05,0.09]	19	[40,42]
12F	1,0	High/intermediate	1,1	440	[0.05,0.09]	6	[40,42]
12M	1,8	Low	1,1	440	[0.025,0.03]	-1	[25,35]
12N	1,3	High/intermediate	1,1	440	[0.05,0.09]	1	[40,42]
12P	1,2	High/intermediate	1,2	200	[0.05,0.09]	14	[40,42]
12Q	1,1	High/intermediate	1,1	440	[0.05,0.09]	1	[40,42]

280A, 280B, 280C, 2671, 267B, 267C, 267D, 268A, 268B, 193A, 193B, 193C, 194A, 194B, 194C, 195A, 195B, 195C, 195D, 195E, 196A, 196B, 196C, 197, 278A,178B, 278C, 317, 279A, 279B, 279C, 318: [8]
11, 10, 8: [7] and [10]
7: [7] and [3]
12B, 12C, 12D, 12E, 12F, 12M, 12N, 12P, 12Q: [9]
* These values have been obtained using the [SII] (6717+6731)/Hα ratios and the [OI] /Hα ratios (in the 4 cases in which we had the [OI] line flux available) and Fig. 3 and Fig. 4 from [6] for the ionization fractions, and Fig.8 and Fig. 9 from [6] for the shock velocities.
** These values have been calculated with the [SII] 6717/6731 line ratios, in addition to Figure 5.3 of [5].
*** In these cases there was no value given for n_0=100 in the theoretical models used.